J Therm Anal Calorim (2012) 109:301–309
DOI 10.1007/s10973-011-1761-9

The influence of alkyl chain length on surfactant distribution within organo-montmorillonites and their thermal stability

Jianxi Zhu · Wei Shen · Yuehong Ma · Lingya Ma · Qing Zhou · Peng Yuan · Dong Liu · Hongping He

Received: 31 May 2011 / Accepted: 16 June 2011 / Published online: 29 June 2011

Abstract Organically modified clay minerals with high thermal stability are critical for synthesis and processing of clay-based nanocomposites. Two series of organo-montmorillonites have been synthesized using surfactants with different alkyl chain length. The organo-montmorillonites were characterized by X-ray diffraction and differential thermogravimetry, combining with molecule modelling. For surfactant with relatively short alkyl chain, the resultant organo-montmorillonite displays a small maximum basal spacing (ca. 1.5 nm) and most surfactants intercalate into montmorillonite interlayer spaces as cations with a small amount of surfactant molecules loaded in the interparticle pores with "house-of-cards" structure. However, for surfactant with relatively long alkyl chain, the resultant organo-montmorillonite displays a large maximum basal spacing (ca. 4.1 nm) and the loaded surfactants exist in three formats: intercalated surfactant cations, intercalated surfactant molecules (ionic pairs), and surfactant molecules in interparticle pores. The surfactant molecules (ionic pairs) in interparticle pores and interlayer spaces will be evaporated around the evaporation temperature of the neat surfactant while the intercalated surfactant cations will be evaporated/decomposed at higher temperature.

Keywords Organo-montmorillonites · Thermal stability · Surfactant · XRD · TG

J. Zhu (✉) · W. Shen · L. Ma · Q. Zhou · P. Yuan · D. Liu · H. He
Key Laboratory of Mineralogy and Metallogeny, Guangzhou Institute of Geochemistry, Chinese Academy of Sciences, Guangzhou 510640, People's Republic of China
e-mail: zhujx@gig.ac.cn

W. Shen · L. Ma · Q. Zhou
Graduate University of Chinese Academy of Sciences, Beijing 100039, People's Republic of China

Y. Ma
Ningbo Institute of Material Technology and Engineering, Chinese Academy of Sciences, Ningbo 315201, People's Republic of China

Introduction

Organically modified clay minerals with high thermal stability are critical for synthesis and processing of clay-based nanocomposites. Hence, during the last decades, a number of studies were conducted using different families of clay minerals and surfactants with different configurations to synthesize organoclays [1–7]. In those studies, most attentions were paid on the thermal properties and the interlayer structure of the obtained organoclays. Various structural models of organoclays have been proposed by using experimental technologies (e.g. XRD, FTIR, NMR, and TEM) [8–14] and molecular modelling methods [15–17]. And their thermal stabilities have been examined by using thermogravimetric analysis (TGA) and differential scanning calorimetry (DSC) [13, 18–25], TGA combined with infrared spectroscopy and mass spectrometry (TGA-FTIR-MS) [26, 27], and TGA combined with pyrolysis/GC–MS [28].

In our recently published paper [6], we have discussed in detail about the influences of montmorillonite's CEC and surfactant configuration on the basal spacing. Therein, we reported that the basal spacing of the organo-montmorillonites increased with surfactant loading, while the maximum basal spacing increased as the alkyl chain length of the surfactant increased. For the same surfactant, the maximum basal spacing of the organo-montmorillonites was little affected by the CEC of the used montmorillonite.

The level of surfactant loading required to reach the maximum basal spacing, however, strongly depended on the CEC. As reported in the literature [14, 29], more than 1 × CEC surfactant was loaded when the maximum basal spacing reached. The surfactant can be loaded by two different styles, i.e., surfactant cations and surfactant molecules (ionic pairs) [30], and they can occupy both the interlayer spaces of clay minerals and the interparticle pores within "house-of-cards" structure [6, 31, 32]. In their thermal stability analyses, the mass loss around the evaporation temperature of the neat surfactant was attributed to the surfactant loaded in the interparticle pores within the "house-of-cards" structure while the mass losses at higher temperatures (except the dehydroxylation) to evaporation/decomposition of the intercalated surfactants [13, 22].

However, in our recent study about organoclays prepared from montmorillonites with different cation exchange capacity and surfactant configuration [6], we found that there were dramatic differences of the mass loss at the similar temperature region for the organoclays prepared from different surfactants. For example, NM-C8-S-4.0 (organoclay prepared from octyl trimethylammonium chloride (C8-S) with an added surfactant of 4.0 times the CEC of montmorillonite) shows a mass loss of 3.25% around 230 °C and 14.21% around 430 °C, the ratio of the former (previously attributed to the evaporation of surfactant in the pores within the "house-of-cards") to the later (previously attributed to the evaporation/decomposition of surfactant in the interlayer spaces) is 0.23. But, for sample NM-C18-S-4.0 (organoclay prepared from octadecyl trimethylammonium bromide (C18-S) with an added surfactant of 4.0 times the CEC) shows a mass loss of 30.48% around 280 °C and 21.34% around 420 °C, the ratio of the former to the latter is 1.43. Such dramatic variation implies that the configuration of the used surfactant has a prominent influence on the location and format of the loaded surfactant and the thermal stability of the resultant organoclay.

To determine the factors affecting the distribution of the loaded surfactant and the thermal stability of organoclays, the organoclays prepared from montmorillonites with different cation exchange capacity and surfactant with different configuration and their thermally treated samples were investigated using X-ray diffraction (XRD) and thermogravimetric analysis (TG), combining with molecular modelling technology. Our present study shows that the alkyl chain length of the used surfactant has a prominent influence on the distribution of the loaded surfactant and accordingly affects the thermal stability of the resultant organo-montmorillonite. Both the surfactants located within the interparticle pores with "house-of-cards" structure and those in the interlayer spaces as ionic pairs will be evaporated around the evaporation temperature of the neat surfactant. The surfactant ionic pairs (molecules) in the interlayer spaces have a significant influence on the basal spacing of organoclays, but they show relatively poor thermal stability when compared with the surfactant cations in the interlayer spaces. These new findings are of high importance for synthesis and application of clay-based nanocomposites.

Experimental

Ca-montmorillonites (NM-Ca) from Inner Mongolia of China was used to synthesize organo-montmorillonite. The purchased montmorillonite sample was dispersed in distilled water with pH ≈ 6–7 by vigorous stirring and the less than 2 μm particle size fractions were collected by sedimenting under gravity. Then, the collected montmorillonite was dried at 105 °C, ground in an agate mortar and passed through a 200-mesh sieve. The obtained sample was stored in a sealed bottle for further use. The cation exchange capacity (CEC), determined by adsorption of $[Co(NH_3)_6]^{3+}$ [33] was 106.5 meq/100 g. The structural formulas for NM-Ca-montmorillonite could be expressed as $(Na_{0.05}Ca_{0.18}Mg_{0.10})[Al_{1.58}Fe_{0.03}Mg_{0.39}][Si_{3.77}Al_{0.23}]O_{10}(OH)_2{\cdot}nH_2O$. The surfactants (99% purity) are octadecyl trimethylammonium bromide (C18-S) and octyl trimethylammonium chloride (C8-S), purchased from Nanjing Robiot Co., Ltd., China. The synthesis procedure of organo-montmorillonite has been depicted in the literature [6].

The thermal treatment of organo-montmorillonites was conducted in a Compact 1,500 °C Tube Furnace (42 mm O. D.) with a temperature accuracy of ±1 °C, at a heating rate of 5 °C/min under pure nitrogen atmosphere (200 mL/min). When reaching the target temperature, the sample was cooled under N_2 in the furnace to room temperature and the product was stored in a sealed bottle for further use. Under such condition, only evaporation and decomposition of surfactant happens rather than oxidation under air. This relatively simple procedure will be helpful for us to well understand the thermal evolution of organo-montmorillonite. The treatment temperatures were determined according to TG–DTG curve of the corresponding original organo-montmorillonite, i.e., the temperatures at which a prominent mass loss occurred or ended. For example, for NM-C18-S-4.0, a prominent mass loss occurs from 162 °C (beginning temperature) to 346 °C (ending temperature), centered at 280 °C. Accordingly, NM-C18-S-4.0 was treated at 162, 280, and 346 °C and the obtained samples were marked as NM-C18-S-4.0-162, NM-C18-S-4.0-280 and NM-C18-S-4.0-346, respectively. The other organo-montmorillonites were thermally treated and marked as the same way.

The original organo-montmorillonites and the corresponding thermally treated products were characterized using XRD and TG techniques. Powder X-ray diffraction patterns (XRD) were recorded between 1° and 20° (2θ) at a step size of 0.0167° using a Bruker D8 Advance diffractometer with Cu K_α radiation (40 kV and 40 mA). Thermogravimetric analysis (TG) was performed on a Netzsch STA 409PC instrument. About 20 mg of finely ground sample was heated in a corundum crucible from 30 to 1,000 °C at a heating rate of 10 °C/min under a pure N_2 atmosphere (60 cm^3/min). The differential thermogravimetric curve was derived from the TG curve automatically. The surfactant loadings in the resultant organo-montmorillonites were determined by using TG curves.

To calculate the interaction between surfactant and montmorillonite, molecular dynamics (MD) simulations were performed using Material Studio (v.5.5, Accelrys, San Diego, USA) and DL_POLY program (version 2.20) [34]. The model of montmorillonite was taken from the experimental study about Ca-montmorillonites from Inner Mongolia. In the montmorillonite model, the isomorphic substitutions obey Loewenstein's rule [35]. The simulation cell consists of two platelets of 32 unit cell each: 8 in *x*-dimension and 4 in *y*-dimension, i.e., an 8 × 4 × 2 super cell. The basal surface area is about 42.24 Å × 36.56 Å. To simplify the calculation procedure and reduce the calculation time, the sample of NM-C18-2.0, which reached the maximum basal spacing as NM-C18-4.0 but contained less surfactants in the resultant organo-montmorillonite, was selected as the model for calculation. For the organo-montmorillonite model, the amount of surfactant cations in the interlayer space was two times the CEC of NM-Ca as determined in experimental measurement. The superfluous positive charges were balanced by Br^-. Water content was determined by thermogravimetric analysis (TG). The model was named as NM-C18-2.0. CLAYFF force field was employed to describe interatomic potentials for the montmorillonite and H_2O components [36]. Interatomic potential for surfactant cations and Br^- was taken from the CVFF force field, the parameters of which were compatible with CLAYFF force field [37]. The combined force field has been successfully used in the simulations of organo-montmorillonite composites. A 15.0 Å cutoff was used for the short-range interaction. The Ewald summation method was used to calculate Coulombic interactions with 3-dimensional periodic boundary conditions. First, simulations were performed in the isothermal-isobaric (NPT) ensemble at 298 k, 1 atm for 1500 ps to achieve equilibrium. Then another 500 ps (NPT) simulations were performed to generate the basal spacing records. A further 500 ps NVT simulation was performed following the previous 2,000 ps NPT simulation to obtain structural properties. In all simulations, the time step was set to be 1.0 fs and all atoms were allowed to move.

Results and discussion

The influences of clay's CEC and the configuration of the used surfactant on the maximum basal spacing of organo-montmorillonite have been extensively discussed in our recently published paper [6]. Our study demonstrates that the organo-montmorillonites prepared from surfactants with two and three alkyl chains show complicated structural and thermal evolutions. Hence, to well understand the influence of alkyl chain length of surfactant on the thermal stability of the resultant organo-montmorillonites, only two series of organo-montmorillonites prepared from octyl trimethylammonium chloride (C8-S, standing for surfactant with relative short alkyl chain length) and octadecyl trimethylammonium bromide (C18-S, standing for surfactant with relative long alkyl chain length) are discussed.

Figure 1 shows XRD patterns of the two series of organo-montmorillonites (NM-C8-S and NM-C18-S) and Fig. 2 shows the loaded surfactant of the resulting organo-montmorillonites prepared at different surfactant concentrations. The surfactant loadings were determined using the TG curves. From Fig. 1, it could be seen that, for the surfactant with relatively short alkyl chain (i.e., C8-S), the basal spacing of the resultant organo-montmorillonite remained at 1.4–1.5 nm despite the increase of the surfactant concentration in the preparation solution. When the surfactant concentration in the preparation solution was lower than 1 × CEC, the amount of the loaded surfactant in the organo-montmorillonite (amount of surfactant in the washed organo-montmorillonite) increased with the increase of surfactant concentration, whereas the loaded surfactant remained unchanged when the surfactant concentration was higher than 1 × CEC. This *d* value suggests that an arrangement of lateral mono-layer model was adopted in the resultant organo-montmorillonite [8, 11]. However, for the surfactant with relatively long alkyl chain (i.e., C18-S), the basal spacing of the organo-montmorillonite increased with the increase of surfactant loading as reported in literature [6, 11, 29]. When the amount of the added surfactant was twice the CEC, the basal spacing reached a maximum (4.1 nm). This *d* value remained constant when the amount of surfactant added exceeded 2.0 × CEC although the loading increased (Fig. 2). As can be seen from Fig. 1, there is a jump of the maximum basal spacing from the organo-montmorillonites prepared from C8-S (1.5 nm) to that from C18-S (4.1 nm), implying that the alkyl chain length of the used surfactant has a significant influence on the local environment of the intercalated surfactant, i.e., the adopted arrangement model and the basal spacing.

When the obtained organo-montmorillonites were examined using thermal analysis, a dramatic difference of the thermal stability was observed. Figure 3 shows TG–

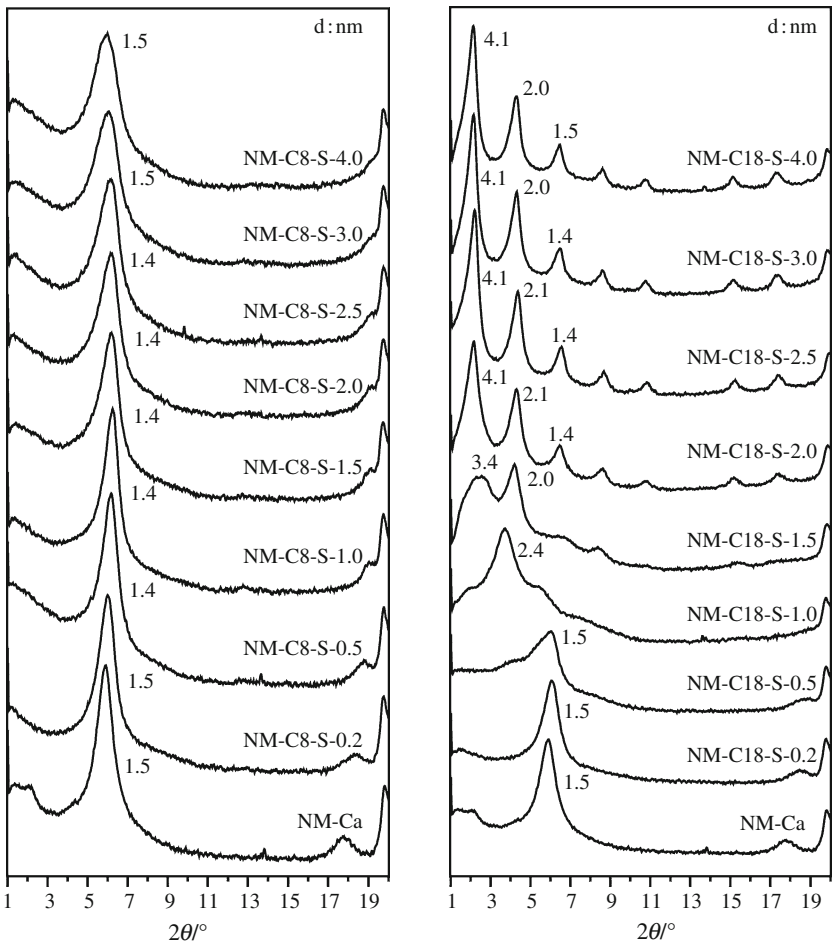

Fig. 1 XRD patterns of two series of organo-montmorillonites (NM-C8-S and NM-C18-S) prepared at different surfactant concentrations

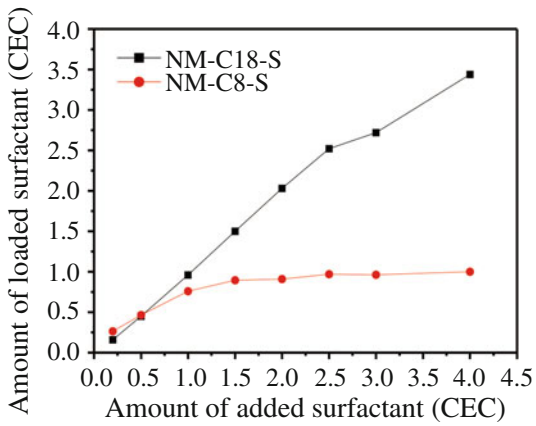

Fig. 2 Loaded surfactant of the organo-montmorillonites prepared at different surfactant concentrations

DTG curves of NM-Ca-montmorillonite, NM-C18-S-4.0, NM-C8-S-4.0 and their thermally treated products. The TG curve of NM-Ca is mainly composed of two parts: (1) the free water (interstitial water and surface adsorbed water) and interlayer water region around 127 °C [38]; (2) the structural water (bonded hydroxyl that undergoes dehydroxylation) region between 600–750 °C. In the temperature range of 200–500 °C, NM-Ca-montmorillonite shows thermal stability without mass loss. Hence, mass loss of organoclays in this temperature range should be attributed to evaporation/decomposition of loaded surfactants.

From TG–DTG curves of NM-C18-S-4.0, it can be seen that the loss temperature and amount of the free water has a prominent decrease, resulted from the surface affinity change (from hydrophobicity to hydrophilicity) of the clay modified with surfactant. Besides the mass loss of free water (ca. 89 °C) and the structural water (ca. 722 °C), two prominent mass loss were recorded at ca. 280 and 410 °C. As NM-Ca-montmorillonite is thermally stable in this temperature range, the mass losses at ca. 280 and 410 °C should be resulted from surfactant evaporation/decomposition of the organo-montmorillonite [13, 39, 40]. However, as shown by the TG–DTG curves of NM-C8-S-4.0, besides the mass losses at ca. 86 and 720 °C, corresponding to the losses of adsorbed water and structural water, a prominent mass loss occurs at 410 °C with a less mass loss at ca. 280 °C. The TG–DTG curve of NM-C8-S-4.0 is obviously different from that of NM-C18-S-4.0.

Previous studies have demonstrated that, under N_2 atmosphere, the mass loss at relatively lower temperature

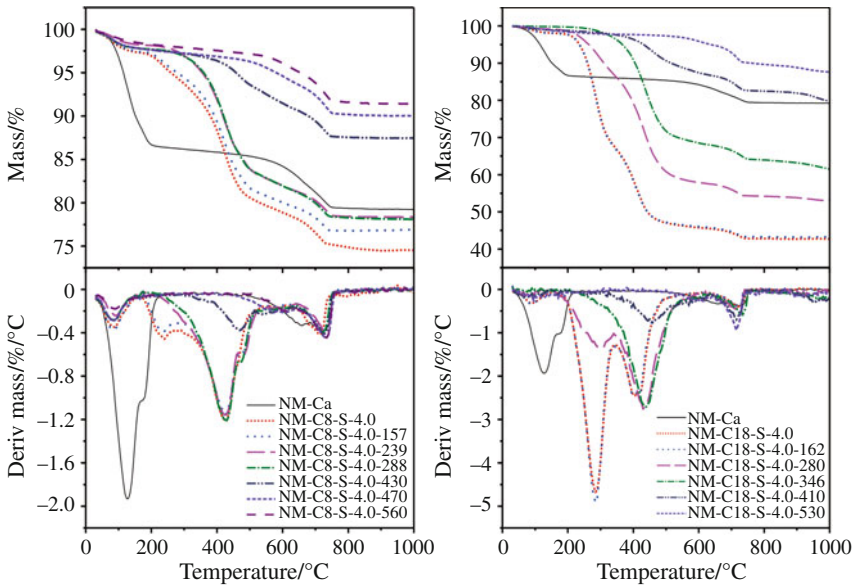

Fig. 3 TG–DTG curves of NM-Ca-montmorillonite, NM-C18-S-4.0, NM-C8-S-4.0, and their thermally treated products

(e.g. 230 °C for NM-C8-S-4.0 and 280 °C for NM-C18-S-4.0 in this study) corresponded to evaporation of the surfactant located in the interparticle pores while that at higher temperature (e.g. ca. 410 °C in this study) to decomposition of the intercalated surfactant [13]. Here, an interesting thing is why so prominent difference of the mass losses at 230–280 and 410 °C is observed in these two series samples.

To determine the location and format of the loaded surfactant and their influence on the microstructural evolution and thermal stability of the organoclay, the thermally treated products from NM-C18-S-4.0 and NM-C8-S-4.0 were investigated by using XRD and TG. The thermal treatment temperatures were adopted according to TG–DTG curves, i.e., the temperatures at which a prominent mass loss began and ended. Accordingly, the treatment temperatures in this study were 162, 280, 346, 410, and 530 °C for NM-C18-S-4.0 and 157, 239, 288, 430, 470, and 560 °C for NM-C8-S-4.0, respectively.

Figure 4 shows XRD patterns of NM-C18-S-4.0, NM-C8-S-4.0 and their thermally treated products. XRD patterns of NM-C18-S-4.0 treated at 162 °C (marked as NM-C18-S-4.0-162) and NM-C8-S-4.0 treated at 157 °C (marked as NM-C8-S-4.0-157) are almost identical to that of the original sample. And the TG–DTG curves of NM-C18-S-4.0-162 and NM-C8-S-4.0-157 are also similar to those of NM-C18-S-4.0 and NM-C8-S-4.0 (Fig. 3). This implies that the thermal treatment at these temperatures does not have any influence on the microstructure of the organo-montmorillonite and almost there is no loss of the loaded surfactant.

For NM-C18-S-4.0, when the treatment temperature increased to 280 °C (marked as NM-C18-S-4.0-280) at which a dramatic mass loss occurred in the TG curve of the original organoclay (NM-C18-S-4.0), the (00 l) reflection peaks were broadened with a slight increase of basal spacing. The TG curve of NM-C18-S-4.0-280 indicates that, after NM-C18-S-4.0 was treated at 280 °C, there is a significant decrease of mass loss around 280 °C, whereas the mass loss around 410 °C remains unchanged (Fig. 3). This treatment temperature (280 °C) is close to the evaporation temperature of the neat surfactant, 269 °C. This suggests that the lost surfactant at ca. 280 °C should be mainly attributed to the surfactant located out of the clay interlayer space, i.e., in the interparticle pores [31, 32] and the broadening of the reflection peaks corresponds to the disordered arrangement of the intercalated surfactant resulted from the thermal treatment. When the treatment temperature further increased to 346 °C, dramatic changes in both XRD pattern and TG curve were observed. As shown by TG–DTG curves (Fig. 3), the mass loss around 280 °C occurring in NM-C18-S-4.0 is not recorded any more in TG–DTG curve of NM-C18-S-4.0-346 whereas the mass loss around 410 °C in NM-C18-S-4.0-280 is identical to that in NM-C18-S-4.0-346. Meanwhile, two broadened peaks with a decreased d value were recorded at 3.42 and 1.41 nm, instead of the regular (001) reflections observed in the original organo-montmorillonite and those treated at 162 and 280 °C. This observation suggests that the mass loss at 162–346 °C corresponds to not only the evaporation of surfactant located in the interparticle pores within "house-of-cards" structure but also the surfactant molecules (ionic pairs) located in the clay interlayer spaces.

When heated to 410 °C, the well-ordered (001) reflections can not be observed and the XRD pattern of NM-C18-S-4.0-410 exhibited a main reflection at 1.34 nm with a broad reflection at 4.57 nm. The corresponding TG–DTG curves showed a significantly decreased mass

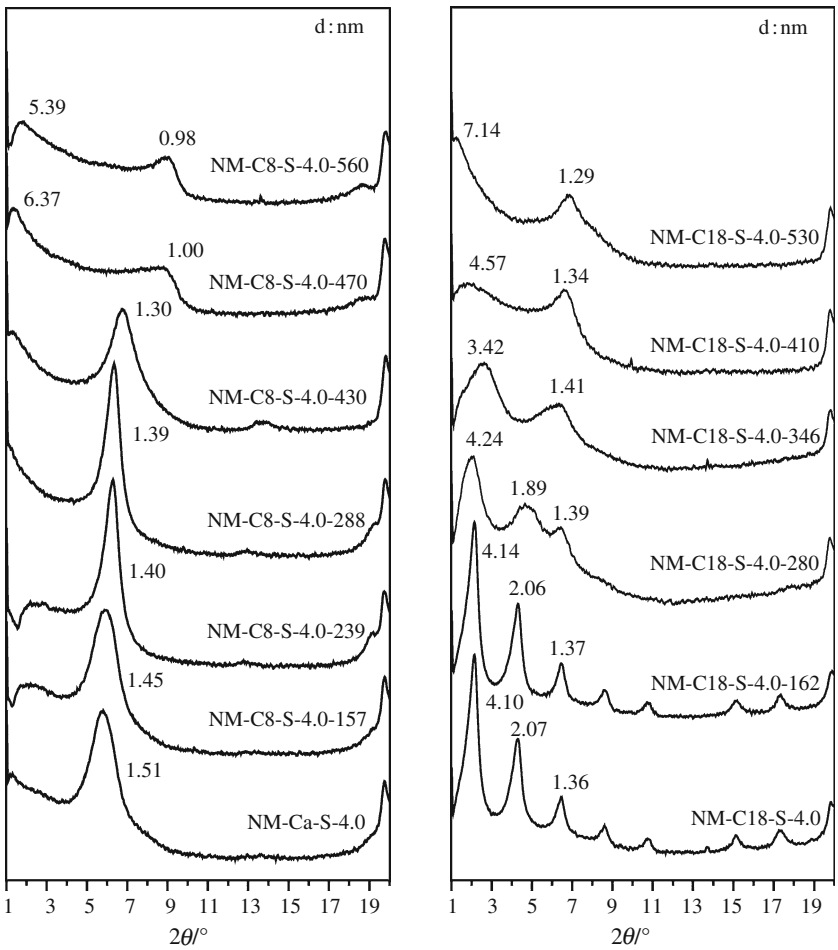

Fig. 4 XRD patterns of NM-C18-S-4.0, NM-C8-S-4.0, and their thermally treated products

loss around 410 °C. When the treatment temperature further increased to 530 °C, the mass loss around 410 °C completely disappeared in the TG–DTG curves and the XRD pattern only exhibited a main reflection at 1.29 nm with a reflection at 7.14 nm. The reflection at 7.14 nm corresponds to the distribution of pores among clay particles [41, 42] while the main reflection at 1.29 nm is similar to that of natural montmorillonite without interlayer water. Here, the dramatic decrease of basal spacing of the thermally treated organo-montmorillonite and the disappearance of mass loss indicate that the mass loss around 410 °C corresponds to the evaporation/decomposition of the cationic surfactant intercalated into the montmorillonite interlayer space. The mass loss around 720 °C should be attributed to the dehydroxylation of montmorillonite.

However, for NM-C8-S-4.0, when the treatment temperature increased to 239 and 288 °C (marked as NM-C8-S-4.0-239 and NM-C8-S-4.0-288), respectively, their TG–DTG curves are almost identical with disappearance of the mass loss at ca. 239 °C in the original sample. Also, their XRD patterns are very similar. This is very different from the results of NM-C18-S-4.0 and their thermally treated products, in which a prominent $d(001)$ decrease was recorded. When the thermal treatment temperature further increased to 430 °C, a dramatic decrease of both the basal spacing and mass loss was recorded. And treated at 470 and 560 °C, only a weak reflection at 1.0 nm was recorded, which is identical to the height of montmorillonite sheet. Also, on their TG–DTG curves, only the mass loss corresponding to the loss of structural water is recorded. Both XRD patterns and TG–DTG curves indicate that the loaded surfactant have been evaporated/decomposed before 470 °C.

From the present study, it can be seen that the configuration of the used surfactant has a prominent influence on the location and format of the loaded surfactants, and their thermal stability and microstructural evolution will be accordingly affected. As shown by the TG–DTG curves (Fig. 3), for sample NM-C8-S-4.0, the mass loss ratio at ca. 239 and 430 °C is 0.23 while that for NM-C18-S-4.0 is 1.43, deduced from the convolution of the DTG curves. The ratio values reflect that more loaded surfactants were evaporated in NM-C18-S-4.0 than that in NM-C8-S-4.0 around the evaporation temperature of the neat surfactant. XRD patterns show that, after NM-C18-S-4.0 treated at 346 °C (the end temperature of surfactant evaporation in

Table 1 Intermolecular interaction energies of surfactant cations and ionic pairs (kcal/mol)

	E (surfactant)	*E* (clay)	*E* (total)	*E* (interaction energy)
Cation	9098.41	−621151.19	−615453.93	3401.14
Ionic pair	5425.77	−621151.19	−616684.53	959.10

the first mass loss step), there is a prominent decrease of the $d(001)$. This implies that some intercalated surfactants are evaporated in this temperature region. As reported in the literature [30], there were two kinds of surfactants intercalated into the clay interlayer spaces: when the amount of the intercalated surfactant is less than the clay's CEC, the surfactants mainly enter into clay interlayer spaces as cations via cation exchange; when the amount of the loaded surfactant is more than clay's CEC, surfactants can enter into clay interlayer spaces as both cations and molecules (ionic pairs) [30] and surfactant molecules also can occupy the interparticle pores within "house-of-cards" structure [32]. It is no doubt that that the surfactants loaded in the interparticle pores will be evaporated around the evaporation temperature of the neat surfactant. In the case of NM-C18-S-4.0, both XRD and TG–DTG suggest that some intercalated surfactants are evaporated around the evaporation temperature of the neat surfactant.

Our calculation of the interaction between surfactant and montmorillonite showed that, in NM-C18-2.0 model, the average spacing was 4.13 nm, which is well consistent with the XRD result (ca. 4.1 nm). In the case of NM-C18-2.0CEC, half of the surfactant was cations while the other half was in the form of ionic pairs. It has been shown that the ammonium head groups of surfactant cations were close to clay mineral surface due to the coulomb interaction in previous simulations [15–17]. The same phenomenon was found in the present simulation. Also, there were some ammonium head groups of surfactant cations lying in the middle of the interlayer spaces, which were accompanied with Br^-, representing the ionic pair form. The confining effects of montmorillonite surface to ions and ionic pairs of surfactant were different. In the molecular simulation, the confining effect can be regarded as intermolecular interaction energy. The intermolecular interaction energy between surfactant and montmorillonite can be calculated by the following equation:

$$E_i = E_s + E_{clay} - E_t$$

E_i is the intermolecular interaction energy between surfactant and montmorillonite; E_s and E_{clay} are single potential energy of surfactant and montmorillonite. E_t is the total potential energy of surfactant and clay mineral. The intermolecular interaction energy between montmorillonite and two forms of surfactant have been calculated as shown in Table 1. The intermolecular interaction energy between surfactant cations and montmorillonite is larger than the ionic pairs of surfactant. This result indicated that the surfactant cations were more strongly confined by montmorillonite surface and harder to escape from the interlayer spaces of montmorillonite. This further confirms our suggestion that the intercalated surfactant molecules (ionic pairs) will be evaporated earlier than those intercalated surfactant cations.

As for the significant variation between the mass loss ratio for NM-C18-S-4.0 (at ca. 280 and 410 °C) and NM-C8-S-4.0 (at ca. 239 and 430 °C), this may be due to the different interlayer spaces for adopting surfactant molecules (ionic pairs). In the case of NM-C18-S-4.0, the montmorillonite interlayer spaces are dramatically expanded from 1.5 nm (original Ca-montmorillonite) to 4.10 nm (NM-C18-S-4.0) and a paraffin bilayer arrangement of the intercalated surfactants was adopted, providing big space for adopting surfactant molecules (ionic pairs). However, in the case of NM-C8-S-4.0, the basal spacing is similar to that of the used Ca-montmorillonite, indicating a lateral monolayer arrangement of the intercalated surfactant [8, 11, 16]. In this case, the space for adopting surfactant molecules (ionic pairs) is limited. In this study, since the same original Ca-montmorillonite was used to prepare organo-montmorillonite, the significant variation between the mass loss ratio for NM-C18-S-4.0 and NM-C8-S-4.0 should be mainly resulted from the obviously different amounts of the surfactant molecules (ionic pairs) in the clay interlayer spaces.

Conclusions

In this study, we prepared two series of organo-montmorillonites using surfactants with different alkyl chain length. In the case of octyl trimethylammonium chloride, a surfactant with relatively short alkyl chain, the obtained organo-montmorillonite only shows a maximum basal spacing at ca. 1.5 nm despite the increase of the surfactant concentration in the preparation solution. The loaded surfactant remained unchanged when the surfactant concentration was higher than $1 \times$ CEC. Most surfactants intercalate into montmorillonite interlayer space as cations with a small amount of surfactant molecules in the interparticle pores within "house-of-cards" structure. For

octadecyl trimethylammonium bromide, a surfactant with relatively long alkyl chain, the resultant organo-montmorillonite displays a large maximum basal spacing at ca. 4.1 nm. The loaded surfactants exist in three formats: intercalated surfactant cations, intercalated surfactant molecules (ionic pairs), and surfactant molecules in interparticle pores. The surfactants loaded in the interparticle pores and intercalated molecules (ionic pairs) are evaporated at a lower temperature than that for evaporation/decomposition of the intercalated surfactant cations. The intercalated surfactant molecules (ionic pairs) have a prominent influence on the increase of basal spacing and the thermal stability of resultant organo-montmorillonite. These new findings are of high importance for synthesis and application of clay-based nanocomposites.

Acknowledgements We gratefully acknowledge financial support from the Knowledge Innovation Program of the Chinese Academy of Sciences (KZCX2-EW-QN101), the National Science Fund for Distinguished Young Scholars (Grant No. 40725006), and the National Natural Science Foundation of China (Grant No. U0933003, 40972034). This is contribution No. IS-1351 from GIGCAS.

References

1. Smith JA, Galan A. Sorption of nonionic organic contaminants to single and dual organic cation bentonites from water. Environ Sci Technol. 1995;29:685–92.
2. Zhu LZ, Chen BL. Sorption behavior of p-nitrophenol on the interface between anion-cation organobentonite and water. Environ Sci Technol. 2000;34:2997–3002.
3. Shen YH. Preparations of organobentonite using nonionic surfactants. Chemosphere. 2001;44:989–95.
4. Yilmaz N, Yapar S. Adsorption properties of tetradecyl- and hexadecyl trimethylammonium bentonites. Appl Clay Sci. 2004;27:223–8.
5. Theng BKG, Churchman GJ, Gates WP, Yuan G. Organically modified clays for pollutant uptake and environmental protection. In: Huang Q, Huang PM, Violante A, editors. Soil mineral microbe organic interactions: theories and applications. Berlin: Springer Verlag; 2008.
6. He HP, Ma YH, Zhu JX, Yuan P, Qing YH. Organoclays prepared from montmorillonites with different cation exchange capacity and surfactant configuration. Appl Clay Sci. 2010;48:67–72.
7. Xue SQ, Pinnavaia TJ. Methylene-functionalized saponite: a new type of organoclay with CH_2 groups substituting for bridging oxygen centers in the tetrahedral sheet. Appl Clay Sci. 2010;48:60–6.
8. Lagaly G. Characterization of clays by organic-compounds. Clay Miner. 1981;16:1–21.
9. Vaia RA, Teukolsky RK, Giannelis EP. Interlayer structure and molecular environment of alkylammonium layered silicates. Chem Mater. 1994;6:1017–22.
10. Lee SY, Kim SJ. Expansion characteristics of organoclay as a precursor to nanocomposites. Colloids Surf A. 2002;211:19–26.
11. Zhu JX, He HP, Guo JG, Yang D, Xie XD. Arrangement models of alkylammonium cations in the interlayer of $HDTMA^+$ pillared montmorillonites. Chin Sci Bull. 2003;48:368–72.
12. He HP, Frost RL, Deng F, Zhu JX, Wen XY, Yuan P. Conformation of surfactant molecules in the interlayer of montmorillonite studied by C-13 MAS NMR. Clays Clay Miner. 2004;52:350–6.
13. He HP, Ding Z, Zhu JX, Yuan P, Xi YF, Yang D, Frost RL. Thermal characterization of surfactant-modified montmorillonites. Clays Clay Miner. 2005;53:287–93.
14. He HP, Frost RL, Bostrom T, Yuan P, Duong L, Yang D, Yunfel XF, Kloprogge JT. Changes in the morphology of organoclays with $HDTMA^+$ surfactant loading. Appl Clay Sci. 2006;31:262–71.
15. Zeng QH, Yu AB, Lu GQ, Standish RK. Molecular dynamics simulation of the structural and dynamic properties of dioctadecyldimethyl ammoniums in organoclays. J Phys Chem B. 2004;108:10025–33.
16. He HP, Galy J, Gerard JF. Molecular simulation of the interlayer structure and the mobility of alkyl chains in $HDTMA^+$/montmorillonite hybrids. J Phys Chem B. 2005;109:13301–6.
17. Heinz H, Vaia RA, Krishnamoorti R, Farmer BL. Self-assembly of alkylammonium chains on montmorillonite: effect of chain length, head group structure, and cation exchange capacity. Chem Mater. 2007;19:59–68.
18. Dana K, Ganguly S, Ghatak S. Thermogravimetric study of n-alkylammonium-intercalated montmorillonites of different cation exchange capacity. J Therm Anal Calorim. 2010;100:71–8.
19. Hrachova J, Billik P, Fajnor VS. Influence of organic surfactants on structural stability of mechanochemically treated bentonite. J Therm Anal Calorim. 2010;101:161–8.
20. Yao C, Ni RJ, Huang Y. Thermogravimetric analysis of organoclays intercalated with the gemini surfactants. J Therm Anal Calorim. 2009;96:943–7.
21. Silva SML, Leite IF, Soares APS, Carvalho LH, Raposo CMO, Malta OML. Characterization of pristine and purified organobentonites. J Therm Anal Calorim. 2010;100:563–9.
22. Yariv S. The role of charcoal on DTA curves of organo-clay complexes: an overview. Appl Clay Sci. 2004;24:225–36.
23. Hedley CB, Yuan G, Theng BKG. Thermal analysis of montmorillonites modified with quaternary phosphonium and ammonium surfactants. Appl Clay Sci. 2007;35:180–8.
24. Sanchez-Martin MJ, del Hoyo C, Dorado C, Rodriguez-Cruz MS. Physico-chemical study of selected surfactant-clay mineral systems. J Therm Anal Calorim. 2008;94:227–34.
25. Zidelkheir B, Abdelgoad M. Effect of surfactant agent upon the structure of montmorillonite X-ray diffraction and thermal analysis. J Therm Anal Calorim. 2008;94:181–7.
26. Xie W, Gao ZM, Liu KL, Pan WP, Vaia R, Hunter D, Singh A. Thermal characterization of organically modified montmorillonite. Thermochim Acta. 2001;367:339–50.
27. Xie W, Gao ZM, Pan WP, Hunter D, Singh A, Vaia R. Thermal degradation chemistry of alkyl quaternary ammonium montmorillonite. Chem Mater. 2001;13:2979–90.
28. Xie W, Xie RC, Pan WP, Hunter D, Koene B, Tan LS, Vaia R. Thermal stability of quaternary phosphonium modified montmorillonites. Chem Mater. 2002;14:4837–45.
29. Li YQ, Ishida H. Concentration-dependent conformation of alkyl tail in the nanoconfined space: hexadecylamine in the silicate galleries. Langmuir. 2003;19:2479–84.
30. Klapyta Z, Fujita T, Iyi N. Adsorption of dodecyl- and octadecyltrimethylammonium ions on a smectite and synthetic micas. Appl Clay Sci. 2001;19:5–10.
31. Wang CC, Juang LC, Lee CK, Hsu TC, Lee JF, Chao HP. Effects of exchanged surfactant cations on the pore structure and adsorption characteristics of montmorillonite. J Colloid Interface Sci. 2004;280:27–35.
32. He HP, Zhou Q, Martens WN, Kloprogge TJ, Yuan P, Xi Y, Zhu JX, Frost RL. Microstructure of $HDTMA^+$-modified montmorillonite and its influence on sorption characteristics. Clays Clay Miner. 2006;54:689–96.

33. Zhu LZ, Zhu RL, Xu LH, Ruan XX. Influence of clay charge densities and surfactant loading amount on the microstructure of CTMA-montmorillonite hybrids. Colloids Surf A. 2007;304: 41–8.
34. Smith W, Forester TR. DL_POLY_2.0: a general-purpose parallel molecular dynamics simulation package. J Mol Graph Model. 1996;14:136–41.
35. Loewenstein W. The distribution of aluminum in the tetrahedra of silicates and aluminates. Am Miner. 1954;39:92–6.
36. Cygan RT, Guggenheim S, van Groos AFK. Molecular models for the intercalation of methane hydrate complexes in montmorillonite clay. J Phys Chem B. 2004;108:15141–9.
37. Dauberosguthorpe P, Roberts VA, Osguthorpe DJ, Wolff J, Genest M, Hagler AT. Structure and enegretics of ligand-binding to proteins—*Escherichia-coli* dihydrofolate reductase trimethoprim, a drug-receptor system. Proteins. 1988;4:31–47.
38. Greene-Kelly R. Dehydration of montmorillonite minerals. Miner Mag. 1955;30:604–15.
39. Xi YF, Zhou Q, Frost RL, He HP. Thermal stability of octadecyltrimethylammonium bromide modified montmorillonite organoclay. J Colloid Interface Sci. 2007;311:347–53.
40. Chen D, Zhu JX, Yuan P, Yang SJ, Chen TH, He HP. Preparation and characterization of anion-cation surfactants modified montmorillonite. J Therm Anal Calorim. 2008;94:841–8.
41. Levitz P, Tchoubar D. Disordered porous solids: from chord distributions to small-angle scattering. Journal De Physique I. 1992;2:771–90.
42. Yuan P, He HP, Bergaya F, Wu DQ, Zhou Q, Zhu JX. Synthesis and characterization of delaminated iron-pillared clay with meso-microporous structure. Microporous Mesoporous Mater. 2006;88: 8–15.